12. A. J. deBold, H. B. Borenstein, A. T. Veress, H. Sonnenberg, *Life Sci.* **28**, 89 (1981).
13. H. Sonnenberg, C. K. Chong, A. T. Veress, *Can. J. Physiol. Pharmacol.* **59**, 1278 (1981).
14. R. Keeler, *ibid.* **60**, 1078 (1982).
15. A. J. deBold, *Proc. Soc. Exp. Biol. Med.* **170**, 133 (1982).
16. _____ and T. G. Flynn [*Fed. Proc. Fed. Am. Soc. Exp. Biol.* **42**, 611 (1983)] described a peptide with 47 residues and a molecular weight of 5273. M. G. Currie *et al.* [*Science* **223**, 67 (1984)] described two peptides with 21 and 23 amino acids, respectively. All three are from rat atria. The last two have also been synthesized. All have natriuretic and diuretic properties.
17. N. C. Trippodo, A. A. Macphee, F. E. Cole, H. L. Blakesley, *Proc. Soc. Exp. Biol. Med.* **170**, 502 (1982).
18. G. Thibault, R. Garcia, M. Cantin, J. Genest, *Hypertension* **5** (Suppl.), I-75 (1983).
19. J. O. Davis *et al.*, *J. Clin. Invest.* **40**, 684 (1961).
20. Both the hamsters and the assay rats were allowed at least 2 weeks to recover from the stress of shipping before they were used. Both had free access to Purina Rat Chow and tap water. The atrial extracts were prepared from two hamsters at the same time to increase the yield. The average atrial weights were 31 and 39 mg for normal and BIO 14.6 hamsters, respectively. Thus the average weights of atrial tissue extracted were 62 mg and 78 mg for normal and BIO 14.6 hamsters, respectively. The extracts were produced in seven pairs, each of normal and myopathic tissue, to eliminate any systematic error that might have occurred if they had all been prepared at the same time.
21. The order of extract preparation was randomized to eliminate any systematic error associated with duration of anesthesia. The extracts were given a number code that was unknown to the person performing the assay to prevent inadvertent bias of the results.
22. The extraction fluid contained 140 m*M* NaCl and 15 m*M* phosphate buffer, *p*H 7.4.
23. M. G. Currie *et al.*, *Science* **221**, 71 (1983).
24. O. H. Gauer and J. P. Henry, *Physiol. Rev.* **43**, 423 (1963); K. L. Goetz, G. C. Bond, D. D. Bloxham, *ibid.* **55**, 157 (1975).
25. F. Karim, C. Kidd, C. M. Malpas, P. E. Penna, *J. Physiol. (London)* **227**, 243 (1972); G. Mancia, J. T. Shepard, D. E. Donald, *Circ. Res.* **37**, 200 (1975); T. C. Lloyd and J. J. Friedman, *Am. J. Physiol.* **233**, H587 (1977); M. D. Thames, *Fed. Proc. Fed. Am. Soc. Exp. Biol.* **37**, 1209 (1978).
26. J. E. Chimoskey, B. A. Breuhaus, S. W. Ely, *Biomater. Med. Devices Artif. Organs* **10**, 2 (1983).
27. C. W. Gottschalk, *Annu. Rev. Physiol.* **41**, 229 (1979).
28. D. C. Fater *et al.*, *Am. J. Physiol.* **242**, H1056 (1982).
29. We thank C. DeLonjay and M. Hamborg-Silver for providing technical assistance, L. Friedsberg and S. Shaft for preparing the manuscript, and Benelisha for assisting us with the ANF literature search. Supported in part by grants from the Michigan Heart Association, the National Science Foundation (PCM 8110588), and the National Institutes of Health (HL01010 and HL07404).

2 December 1983; accepted 4 January 1984

Microdifferential Holography and the Polysarcomeric Unit of Activation of Skeletal Muscle

Abstract. *Unbalanced holographic difference images of contracting skeletal muscle fibers reveal that activation affects the amplitude of the light scattered by individual myofibrils. The results suggest that the unit of activation is not the sarcomeric structural unit, but a monomyofibrillar segment containing 20 to 40 contiguous sarcomeres.*

For nearly two decades holographic interferometry has been the method of choice for analyzing the deformations of inanimate objects under stress (*1*, *2*). More recently the method has found its way into macroscopic biomechanics (*3*), but it has not been widely recognized that, with suitable modification, holographic interferometry can provide insight into the microscopic concomitants of the elementary life processes themselves. The power and potential scope of holographic methods in physiology are suggested by the novel images of contracting muscle presented in this report.

In our experiments isolated fibers or fiber pairs dissected from frog semitendinosus muscle were mounted on a microscope stage in Ringer solution at room temperature and transilluminated by a laser beam with a wavelength of 514.5 nm. Light passing through the microscope, the object wave, was directed to a holographic plate that was also illuminated by a coherent, collimated reference wave. The plate was doubly exposed by a pair of light flashes, submillisecond in duration, separated by 25 msec. During this interval the optical path traversed by the reference wave was shortened by a half-wavelength (*4*). Images reconstructed from such holograms reveal only the difference between the images that would be reconstructed from either exposure alone. Bright areas in such images may originate in submicroscopic motion of small structures, in gross translation, or in changes in the shape or index of refraction of the specimen. Differential control images of resting fibers proved vacuous, as expected, while nondifferential control images obtained without shortening the reference path were of normal appearance (Fig. 1A). When stimulated by pulses of transverse electrical current the fibers exhibited sharp response thresholds. The isometric tension curves, which peaked at about 10^5 N/m^2, were stable and repeatable for many hundreds of twitches. When carefully stored the fibers retained

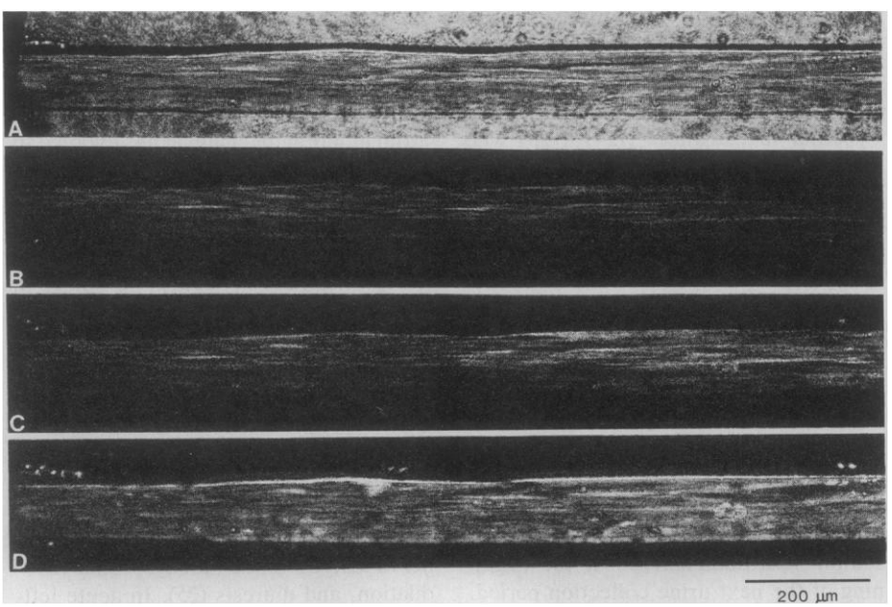

Fig. 1. Holographic images of a portion of a fiber viewed through a ×10 microscope objective lens (numerical aperture, 0.30). The microscope was focused on the plane in which the lower edge of the fiber appeared sharp. Illumination was in the equatorial plane, passing obliquely at numerical aperture 0.22 from the lower portion of the field of view toward the upper portion. The upper edge of the fiber is therefore in partial shadow. The fiber was stimulated by 0.2-msec pulses of current between a pair of point electrodes lying immediately above and below the field of view near its left edge (fiber diameter, 90 μm; striation spacing, 2.7 μm; temperature, 22°C; and exposure length, 0.5 msec). (A) Nondifferential image of resting fiber. The three bright spots at the shadow's left edge and the four similar spots at extreme upper right are blood corpuscles or bits of capillary tissue closely applied to the fiber's surface. These seven spots are weakly imaged in (C) and brightly double-imaged in (D). (B to D) Differential images of the same portion of the fiber, stimulated at successively earlier times during the interval between exposure flashes. Background and static portions of the fiber and capillary tissue have been holographically subtracted from the images and appear black. Apart from the fourfold overexposure used to "burn in" the very bright image in (A), the holographic and photographic exposure and development parameters were the same for all four images.

these characteristics for several days after their use for holography. Typically, four holograms were made under any one set of conditions, with generally consistent results.

Images of a fiber at rest and in the early stages of contraction are shown in Fig. 1. In Fig. 1B, where the second holographic exposure flash coincided very nearly with the onset of active tension, the image reveals only submicroscopic motion, apparently at the myofibrillar level (*5*). Such features are absent from images made only 0.5 msec earlier in the contraction cycle. In the image in Fig. 1C, made 0.5 msec later than that in Fig. 1B, these features are brighter but not longer or more numerous; the blood corpuscles visible in Fig. 1A here acquire brightness due to a slight longitudinal displacement of the entire fiber. In the image in Fig. 1D, made 3 msec further into the contraction cycle, the displacement that occurred between exposures has become sufficient to cause each corpuscle to appear twice. The distance between the doubled images corresponds to 15 μm on the left and 10 μm on the right. It is noteworthy that, despite the contraction which has taken place,

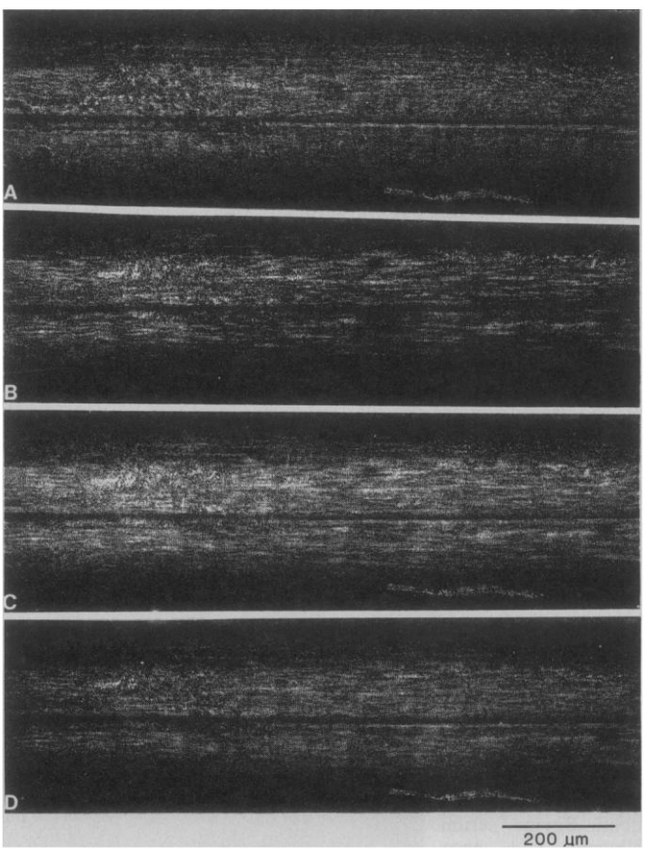

Fig. 2. Holographic images of a fiber pair. The microscope carried a ×10 objective lens (numerical aperture, 0.30) focused on the plane in which the lower edge of the lower fiber appeared sharp. This edge is crisply reproduced in reconstruction from nondifferential holograms (not shown). Lying in the same plane, parallel to and equidistant from the fibers, were a pair of long, fine stimulating electrodes. The anode lay about 2 mm below and the cathode about 2 mm above the imaged area. Illumination is in the meridional plane, passing obliquely at numerical aperture 0.22 from the right-hand portion up toward the left-hand portion of the field of view. Fiber diameters in the slack condition were both 125 μm. Here the striation spacing is 2.8 μm. (A) Differential image of fibers during rest, obtained under positive unbalance. Negatively unbalanced images of the resting fibers were identical to this one in appearance and intensity. The bright object at bottom right is a wisp of cotton that adhered to the specimen throughout the experiment. (B) Balanced differential image of the stimulated fibers, made near the onset of active tension. The amplitudes of the bright filaments, many of which cannot be discerned in (A), are comparable to or somewhat larger than the residual amplitudes in (A). The wisp of cotton does not appear here, indicating that the fibers are not in motion. (C) Positively unbalanced differential image of the fibers when stimulated as in (B). The bright filaments in (B) interfere constructively with the residual image (A) and are highly visible, even though their surround is much brighter than in (B). (D) Negatively unbalanced differential image of the fibers when stimulated as in (B) and (C). There is partial destructive interference between the bright filaments (B) and the residual image (A). Many of the filaments are nearly invisible, and many that are not less bright than in (B). Except for the conditions of balance, holographic and photographic protocols were the same for all images.

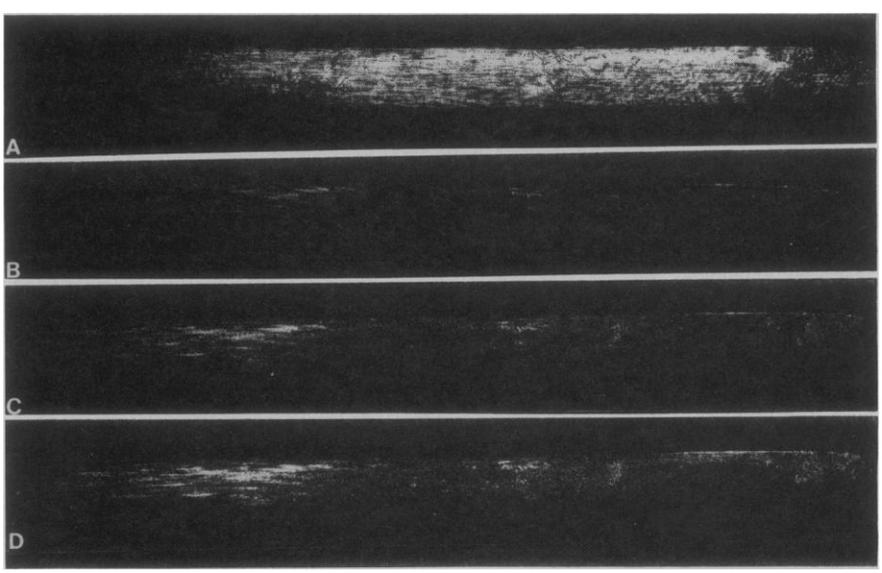

Fig. 3. Holographic images of the earliest activation in a fiber, a 2.5-mm portion of which was viewed through a ×6.3 objective (numerical aperture, 0.20). The microscope was focused on the plane in which the upper edge of the fiber appeared sharp. The geometries of illumination and stimulation are the same as those in Fig. 2. The fiber was 10.1-mm long when almost slack and was mounted at this length (fiber diameter, ~ 150 μm; striation spacing, 2.07 μm; temperature, 25°C; and exposure duration, 0.2 msec per flash). (A) Nondifferential image of resting fiber. (B to D) Differential images of the same portion of the fiber, stimulated at successively earlier times during the interval between exposure flashed. The massive stimuli were single current pulses 0.2 msec long and had a strength 1.4 times threshold. They were advanced 0.2 msec between successive frames. Apart from the overexposure used to burn in the image in (A), holographic and photographic procedures were the same for all four images. The filamentary features nucleate in three discrete areas on the cathode side of the fiber and the brightening propagates inward with a velocity ranging from ~ 10 cm/sec on the right to ~ 25 cm/sec on the left. [The results of Gonzales-Serratos (*7*), extrapolated to 25°C, predict a velocity of ~ 10 cm/sec.] Note that brightening of the edge on the anode side appears to be inhibited and that the spread of brightness in the longitudinal direction is not much faster than that which occurs radially. The dark areas remaining in (D) brighten very rapidly during the next 0.6 msec of the contraction cycle.

each of the filamentary features that cropped up in Fig. 1B survives, its brilliance largely undiminished and still uniform. Such uniformity suggests that the features arose through displacement, as did the brightening corpuscles in Fig. 1C.

The inadequacy of this attractively simple explanation is pointed out by an experiment based on the fact that light scattered by a rigidly displaced object changes in phase but not in amplitude. Two unbalanced differential holograms are made, one positively unbalanced with the first flash 30 percent longer than the second flash (which is fixed in length), the other negatively unbalanced with the first flash 30 percent shorter. The two object waves reconstructed from either of these holograms interfere destructively, but incompletely so: the resultant image amplitudes of a resting fiber would be, uniformly, +0.3 or −0.3 times as great as those reconstructed from a hologram exposed by the second flash alone, according to the sign of the unbalance. If activation evoked changes in the amplitudes of the waves scattered by the myofibrils, these changes would interfere constructively or destructively with the residual wave created by unbalancing the exposure flashes. The myofibrils would then appear more brightly in one of the two unbalanced holographic images than in the other. On the other hand, if phase shifts in their scattering were the sole source of the bright filaments in the balanced images, the myofibrils would be equally visible in the two unbalanced images.

The results of such an experiment are depicted in Fig. 2. Without exception, the myofibrils scatter less light after activation of the fiber than before. In the case illustrated the scattering amplitudes have diminished rather uniformly by 30 percent or more. This reduction is the principal cause of the bright filamentary features in the balanced image.

The reduction in myofibrillar scattering persists in unbalanced images made sufficiently beyond the advent of contraction that shortening is readily measurable. Yet we have never succeeded in eliciting it while the myofibrils under observation were responding only passively to activation elsewhere in the fiber (*6*). This phenomenon must, therefore, be a concomitant of the activation of the myofibrils themselves. Indeed, when the development of the pattern of filamentary brightness in a fiber is examined under greater time resolution than in Fig. 1, it is found (Fig. 3) to nucleate in the depolarized portion of the sarcolemma and to propagate inward at a speed consistent with that already known to characterize the inward spread of activation (*7*).

Nonetheless, it may be questionable whether the bright filaments in our photographs are actually images of myofibrils. Nuclei present in the fibers have dimensions comparable to those of some of our filaments (*5*), and although normally the sarcoplasmic reticulum (SR) is not optically resolvable (*5*), changes in its structure might contribute differential brightness. It is known (*8*) that nuclei and mitochondria comprise about 1.6 percent, SR about 9 percent, and myofibrils about 83 percent of the volume of frog semitendinosus fibers. Were the 9 percent of the volume occupied by the SR to reduce the scattering amplitude 30 percent or more, the SR would have to be a major determinant of the appearance of the resting fiber. Serious disruption of the SR, such as occurs during prolonged extraction with 50 percent glycerol (*9*), would then seriously disrupt the myofibrillar and sarcomeric pattern of the fiber. Experimentation confirms, however, that the myofibrillar pattern can be preserved intact during such extraction (*10*). It follows that changes in the SR cannot be the dominant source of our bright filaments. On the other hand, the ubiquity of the bright filaments shows that they cannot all have been associated with nuclei: the bright filaments must be images of myofibrillar material.

We supported and refined this conclusion by adding enough bovine serum albumin to the Ringer solution to match its index of refraction with the average index of the fiber (*11*). This precaution practically eliminates the spherical aberration and astigmatism that otherwise result from refraction at the surface of the fiber and produces micrographs of superior clarity in which the myofibrils lie manifestly parallel to the fiber axis. The behavior of a fiber in such circumstances (*12*) is shown in Fig. 4. The diameters of the myofibrils in the nondifferential image (Fig. 4B) are comparable with those found in other observations (*5, 11*) of frog muscle, and there is great conformity between the bright filaments of the differential image (Fig. 4A) and corresponding portions of the nondifferential myofibrillar pattern of the resting fiber. The bright filaments are evidently segments of single myofibrils. They are strikingly discrete: not every myofibril appears to be active, and most of those that are occur well isolated from other active myofibrils. The onset of activation is thus a fundamentally monomyofibrillar process. The large, abrupt, segmental reduction in scattering amplitude that accompanies it, becoming fully estab-

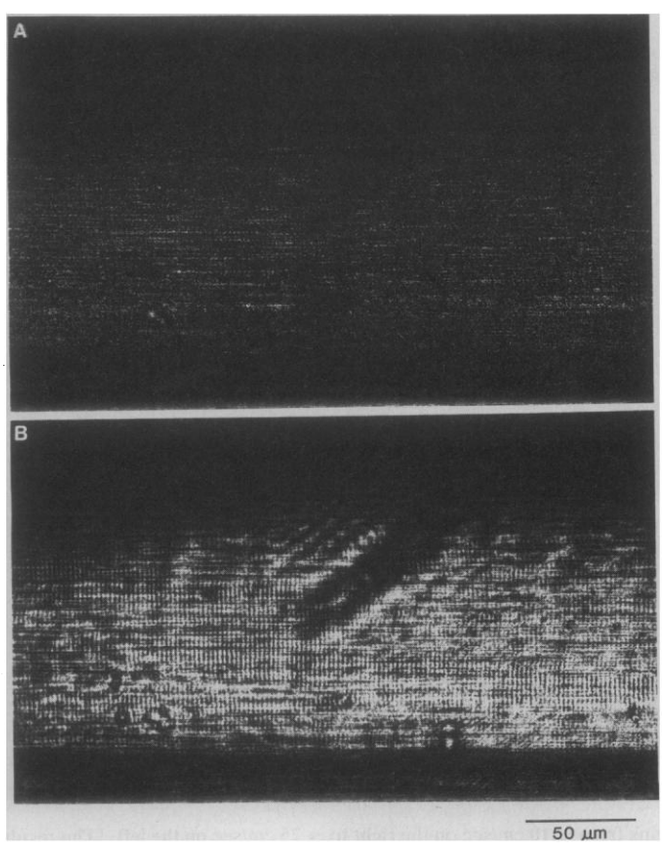

Fig. 4. Holographic images of a fiber viewed by a ×40 water-immersion objective (numerical aperture, 0.75) focused on the upper edge of the fiber. Bovine serum albumin had been added to the Ringer solution (fiber diameter, 125 μm and striation spacing, 2.05 μm). (A) Differential image made near the onset of active contraction. Unbalanced images, not shown, demonstrate that the bright filaments visible here arose from reductions in their scattering amplitudes of about 30 percent. (B) Nondifferential image of the same region of the resting fiber. Image has been burned in by overexposure. The dark circular arcs, top center, are the shadows of a smudge on the bottom of the specimen chamber. The bright vertical crossstriations are imaged as dark lines in (A).

lished within 0.5 msec of its inception (*13*), must reflect the rearrangement of highly polarizable macromolecules in a fashion that is both submicroscopic and uniform or uniformly periodic along a myofibrillar domain with a mean length of eight sarcomeres in the specimen shown.

This is an unexpected result. Electron microscopy of fixed and stained specimens teaches that the structural unit of striated muscle is not the myofibril, but the sarcomere (*5*). Each sarcomere is invested with longitudinal and transverse SR elements (*14*), and these elements are in communication, at the level of each sarcomere, with the transverse tubular T system, which communicates to the interior of the fiber the depolarization conveyed by the action potential along the sarcolemma (*15*). The invaginations of the sarcolemma giving rise to the T tubules (*16*) have the same longitudinal spacing as the sarcomeres themselves (*16, 17*). On the basis of such structural periodicity, it might be expected that, as the action potential sweeps over the sarcolemma and inward through the T system, the activation that breaks out in its wake would be synchronous or stochastic. If it were stochastic, individual structural units randomly located in the wake would develop activity randomly in time. Successive differential images of the process would have a "salt-and-pepper" appearance until a large fraction of all structural units had become active. In synchronous activation contiguous structural units would become uniformly and simultaneously active over polymyofibrillar regions of length $v_s\Delta t \simeq 400$ μm and breadth $v_r\Delta t \simeq 20$ μm, where v_s (~ 140 cm/sec) and v_r (~ 7 cm/sec) are the axial (17°C) (*18*) and radial (20°C) (*7*) velocities of propagation of the action potential, respectively, and Δt is the time resolution of the observation (~ 0.2 msec in Fig. 3). Neither of these expected outcomes is compatible with our holographic images, which show that the activation that first appears is both segmental and sparse.

Departures from the idealized structures we have sketched are known. Among them are occasional longitudinal elements (*19*) and culs-de-sac in the T system (*20*) and helicoids in both the T system and the sarcomeric registration (*20*). The longitudinal elements and culs-de-sac are very short (*19*) and the helicoids may attain lengths of eight striations longitudinally, but all these irregularities are far less numerous (*20*) than our bright filaments. Thus a proper accounting for the segmentalization appears more likely to be found at the level of the myofibrillar dynamics, or possibly in the distribution of transport in the SR or T systems, than at the level of static structure. A hint that its origin may, with pharmacological assistance, prove identifiable is furnished by our finding that the exposure of a fiber to Ringer solution containing bovine serum albumin not only alters the temporal course of its activation (*12*) but also markedly shortens the filaments that shine in its differential images.

M. SHARNOFF
T. H. KARCHER
L. P. BREHM

Department of Physics, University of Delaware, Newark 19711

References and Notes

1. R. L. Powell and K. A. Stetson, *J. Opt. Soc. Am.* **55**, 1593 (1965).
2. L. O. Heflinger, R. F. Wuerker, R. E. Brooks, *J. Appl. Phys.* **37**, 642 (1966).
3. A representative set of applications can be found in G. von Bally, Ed., *Holography in Medicine and Biology* (Springer-Verlag, Berlin, 1979).
4. M. Sharnoff, R. W. Henry, D. M. J. Bellezza, *Biophys. J.* **21**, 109a (1978).
5. An informative collection of definitions, drawings, and photographs is given by D. S. Smith [*Muscle* (Academic Press, New York, 1972)].
6. This situation can be produced by stimulating a fiber locally at one end and observing the other end before its invasion by the action potential. In our experiments this created an interval of several milliseconds during which the myofibrils at the unstimulated end were being passively stretched by the active contraction of those at the stimulated end (*18*).
7. H. Gonzales-Serratos, *J. Physiol. (London)* **212**, 777 (1971).
8. B. A. Mobley and B. R. Eisenberg, *J. Gen. Physiol.* **66**, 31 (1975).
9. J. R. Bendall, *Nature (London)* **170**, 1058 (1952).
10. J. Borejdo and S. Putnam, *Biochim. Biophys. Acta* **459**, 578 (1977).
11. A. F. Huxley and R. Niedergerke, *J. Physiol. (London)* **144**, 403 (1958).
12. L. Hill, *ibid.* **266**, 677 (1977).
13. This is shown in Figs. 1 and 3 and is confirmed by unbalanced images made as in Fig. 2 but later during contraction. The process requires only about 1 percent of the time required for peak tension to develop during a twitch.
14. L. D. Peachey, *J. Cell Biol.* **25**, 209 (1965).
15. J. Bastian and S. Nakajima, *J. Gen. Physiol.* **63**, 257 (1974).
16. C. Franzini-Armstrong, L. Landmesser, G. Pilar, *J. Cell Biol.* **64**, 493 (1974).
17. A. F. Huxley and R. E. Taylor, *J. Physiol. (London)* **144**, 426 (1958).
18. P. Fatt and B. Katz, *ibid.* **115**, 320 (1951).
19. B. Eisenberg, *J. Cell Biol.* **55**, 68a (1972).
20. L. D. Peachey and B. R. Eisenberg, *Biophys. J.* **22**, 145 (1978).
21. Supported by the University of Delaware Research Foundation and by NSF grant BNS 7822199.

9 April 1983; accepted 29 December 1983

Functional Expression of a Cloned I-Aβ^k Gene in B-Lymphoma Cells

Abstract. *The immune response genes of the mouse encode two cell-surface glycoproteins, I-A and I-E, that play critical roles in determining the animal's immune responsiveness. The I-A antigen contains two chains, α and β. A cloned β-chain gene, I-Aβ^k, was introduced into B-lymphoma cells that express I-A^d. The transfected gene was successfully expressed on the cell surface of the recipient cells and was functional in stimulating allospecific T cells.*

The I-region of the major histocompatibility complex (MHC) of the mouse encodes the I-A and I-E polymorphic cell-surface glycoproteins referred to as Ia antigens or class II antigens. Each Ia antigen consists of three noncovalently linked polypeptide chains—the α (~ 34 kilodaltons), β (~ 28 kilodaltons), and the invariant chain (~ 30 kilodaltons) (*1*). Ia antigens are expressed primarily on B cells and on antigen-presenting cells such as macrophages and dendritic cells and play a major role in cell-cell interaction and in regulation of the immune response (*2*). To gain a better understanding of the mechanism of Ia antigen regulation, we introduced genes encoding the I-A antigen into mouse B-lymphoma cells. We now report the successful expression of transfected I-Aβ^k (*3*) gene product on the cell surface of antigen-presenting B-lymphoma cells. The expressed I-Aβ^k chain was functional in stimulating allospecific T cells.

Genes of class I antigens of the MHC have been successfully transfected into L cells. Transfected class I genes were expressed on the cell surface of L cells and were able to function as restriction elements in T-cell–specific cytotoxic responses against viruses (*4, 5*). Expression of a functional Ia antigen from transfected class II MHC genes presented a more difficult problem. Although Ia genes can be expressed in L cells (*6, 7*), they are not fully functional. Therefore, we introduced the cloned I-Aβ^k gene into BALB/c B-lymphoma cells M12.4.1 and A20.2J (*8*), which express I-A^d-encoded antigens and are potent Ia-restricted antigen-presenting cells (*9*). These cells should have all the machinery necessary to assemble functional I-A antigens. The successful transfection of M12.4.1 and A20.2J cells with the I-Aβ^k gene should result in a hybrid I-A$^{k/d}$ molecule formed by the pairing of the I-A^d α chain from the B-lymphoma cell with the transfected I-A^k β chain.

The I-Aβ^k gene was introduced into B